

# Studies on the Influence of Formulation and Processing Factors on the Drug Release from Multiparticulate Systems

K. V. R. N. S. Ramesh, Hemant Kumar Singh Yadav, Shahnaz Usman,  
Tamer Salama Elmarsafawy

Department of Pharmaceutics, RAK College of Pharmaceutical Sciences, RAK Medical and Health Sciences University, Ras Al Khaimah, United Arab Emirates

## Abstract

**Background:** Multiparticulate delivery systems are being increasingly recognized as more beneficial over single unit products because of more uniform distribution in gastrointestinal tract, less chance of dose dumping, better control on drug release, and more bioavailability with negligible variation among different individuals. Pellets are one commonly employed multi-particulate dosage form. New polymers need to be explored for their utility in palletization process. **Objective:** The goal of the investigation is to assess the feasibility of employing inclusion complex of poorly soluble drug furosemide in the design of slow-release pellets and investigate the usefulness of almond gum as a pelletizing agent. **Materials and Methods:** Inclusion complex of furosemide in sulfobutyl ether- $\beta$ -cyclodextrin is prepared to enhance its dissolution. Pellets of inclusion complex are prepared by extrusion and spheronization employing almond gum as the spheronizing agent. The influence of almond gum proportion and speed of spheronization on the characteristics of pellets and drug release is investigated. **Results:** Inclusion complexation converted crystalline furosemide into an amorphous form, enhancing its dissolution. With changes in the percentage of almond gum and speed of spheronization, the size of the pellets could be varied which ranged from 640 to 1305  $\mu$ . **Conclusion:** Employing the inclusion complex of poorly soluble drugs for preparing SR pellets is a novel approach which ensures prompt, but slow-release spread over 12 h in the gastric fluids.

**Key words:** Dissolution, drug release, inclusion complex, pellets, spheronization

## INTRODUCTION

New technologies and processes are being developed for existing and new drug molecules to prepare sustained-release (SR) and controlled release (CR) dosage forms. SR or CR dosage forms offer advantages over the conventional immediate-release dosage forms.<sup>[1,2]</sup> Most approaches in the design of SR dosage forms aim to prepare single unit forms such as matrix tablets. However, the multi-unit forms such as microcapsules, microspheres or pellets offer significant advantages such as better control over drug release, less chances of dose dumping, and a more uniform distribution in the entire gastrointestinal tract after oral administration leading to uniform and rapid onset of absorption process.<sup>[3,4]</sup> Among the multi-unit forms, pellets are one of the most popular multi-particulate dosage forms. Palletization is process that transforms fine powders of active drug substances or additives into well-rounded units

called pellets that have good flow characteristics. The size of pellets varies from 0.5 mm to 1.5 mm.<sup>[5]</sup>

Out of the various methods employed to prepare pellets, extrusion and spheronization is a widely employed technique to manufacture pellets. Sandipkumar *et al.* developed CR domperidone pellets.<sup>[6]</sup> They employed microcrystalline cellulose (MCC) as the core seed to prepare the modified release pellets. Lipophilic calcium stearate pellets of ibuprofen for CR were developed by Roblegg *et al.*<sup>[7]</sup>

### Address for correspondence:

K. V. R. N. S. Ramesh, Department of Pharmaceutics, RAK College of Pharmaceutical Sciences, RAK Medical and Health Sciences University, Ras Al Khaimah, United Arab Emirates. Phone: 00971503716203. E-mail: venkatramesh@rakmhsu.ac.ae

**Received:** 13-09-2019

**Revised:** 03-11-2019

**Accepted:** 11-11-2019

In most extrusion and spheronization methods, MCC is widely used as the spheronizing agent. Despite its good attributes to aid in the process of spheronization, other agents are being increasingly investigated for their utility. This is because of reported chemical and physical incompatibilities of drugs with MCC.<sup>[8,9]</sup> Several workers reported on the preparation of pellets employing other spheronizing agents such as xanthan gum, chitosan, and polyvinyl alcohol.<sup>[10-12]</sup> In this investigation, we explored the usefulness of almond gum in the development of pellets by extrusion and spheronization. Almond gum is exudate obtained from the plant *Amygdalus communis*.<sup>[13]</sup> There are some reports on the binding and release retarding properties of almond gum, and it is reported to be useful in the preparation of hydrogel silver nanoparticles.<sup>[14,15]</sup>

Pellets prepared by extrusion/spheronization employing almond gum were investigated for SR of furosemide used as a model drug. Furosemide, a poorly soluble drug as per the biopharmaceutical classification system (BCS), is a diuretic agent that is used in the treatment of hypertension and edema associated with heart failure.<sup>[16]</sup> For the successful development of an SR dosage form, it is essential that the technology developed is suitable for the drug involved. Because the development of SR dosage forms for poorly soluble BCS Class IV drugs is very challenging. BCS Class IV drugs have poor solubility and permeation characteristics.<sup>[17]</sup>

Developing SR dosage forms for poorly soluble drugs is challenging because drug release promptly from the product depends on the drug dissolution. In this regard, it is anticipated that difficulties may be encountered to design slow-release products for the relative water-insoluble drugs such as furosemide. Since furosemide exhibits low solubility in gastric fluids, to initiate a prompt release from the pellets, a novel approach of incorporating the inclusion complex of furosemide in sulfobutyl ether- $\beta$ -cyclodextrin (SBE<sub>7</sub>- $\beta$ -CD) in almond gum pellets was explored. SBE<sub>7</sub>- $\beta$ -CD is a modified  $\beta$ -cyclodextrin that has better drug entrapment ability, better physical and chemical properties than the parent cyclodextrin. It is reported to be having high solubility (excess 70 g/100 ml) and minimal toxicity.<sup>[18,19]</sup> SBE<sub>7</sub>- $\beta$ -CD, which is being explored in the development of injectable products and found to be useful to stabilize drugs, is reported to be safe after intensive chronic safety evaluation.<sup>[20]</sup>

## MATERIALS AND METHODS

Furosemide (gift sample from Julphar Gulf Pharmaceutical Industries UAE), SBE<sub>7</sub>- $\beta$ -CD (SBE<sub>7</sub>- $\beta$ -CD-Cydex Corp, USA); Almond Gum (Grade 1) is procured from Hare Krishna Herbals, Kakinada, India. All other excipients, chemicals, and solvents are of analytical grade and were purchased commercially.

## Inclusion complexation of furosemide in SBE<sub>7</sub>- $\beta$ -CD

### Phase solubility study

Phase solubility studies were done to know the molar ratio of complex formation between furosemide and SBE<sub>7</sub>- $\beta$ -CD as per the Higuchi and Connors method.<sup>[21]</sup>

Excess amounts of furosemide were added to 15 ml of distilled water containing increasing concentrations of SBE<sub>7</sub>- $\beta$ -CD in 25 ml stoppered glass bottles. The resulting dispersions were shaken at  $37 \pm 0.5^\circ\text{C}$  for 3 days in a temperature-controlled shaking water bath (SeichemTech SK 330 Pro). At the end of 3 days, sample dispersion was removed and after filtration through a  $0.45 \mu\text{m}$  membrane, estimated spectrophotometrically at 271 nm (Shimadzu Model UV 1600) for the amount of furosemide soluble.

Phase solubility studies were performed in triplicate. Solubility diagrams were drawn between the molar concentration of furosemide soluble and the molar concentration of SBE<sub>7</sub>- $\beta$ -CD. From the resulting plot, the stability constant for the formation of complex between furosemide and SBE<sub>7</sub>- $\beta$ -CD was determined by employing the formula:

$$K_s = \text{Slope}/S_0(1-\text{Slope})$$

The slope is calculated from the plot [Figure 1] and  $S_0$  is the equilibrium solubility of furosemide.

### Preparation of inclusion complex

The inclusion complexes of furosemide with SBE<sub>7</sub>- $\beta$ -CD were prepared by kneading (KN) and freeze-drying (FD) procedures in a 1:1 M ratio.

### KN method

The required quantities of furosemide and SBE<sub>7</sub>- $\beta$ -CD were accurately weighed, added to a mortar, and kneaded for 45 min. While carrying out the KN, little quantity of methanol:water (20:80 v/v) solution was added to the kneaded mass to ensure sufficient consistency. The mass obtained was

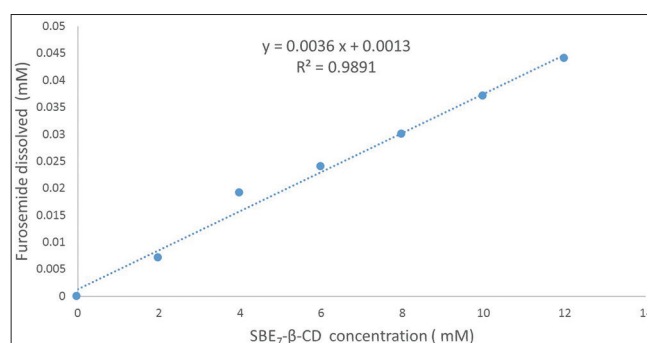


**Figure 1:** Phase solubility diagrams of furosemide with sulfobutyl ether- $\beta$ -cyclodextrin

dried at 40°C for 48 h, powdered, and then passed through a 100-mesh sieve and stored until further use.

### FD method

Appropriate amounts of furosemide and SBE<sub>7</sub>-β-CD were dissolved in methanol (8 ml) and water (32 ml), respectively. The aqueous and methanolic solutions were then mixed for 24 h at 25°C using a magnetic stirrer. The blended solution was subjected to freezing at -70°C and latter FD for 48 h at -50°C using a FD (SP Scientific, Model PRO 3XL). The FD powder was sifted through a 100-mesh sieve and stored until further use.

## Evaluation of inclusion complexes

### Dissolution

The dissolution pure drug furosemide of the complexes was studied using United States Pharmacopoeia (USP) Type II dissolution rate test apparatus (Lab India Model DISSO). Furosemide or its complexes equivalent to 10 mg of furosemide were added to 900 ml of dissolution medium (0.1 N hydrochloric acid). The paddle was operated at 50 rpm and temperature was maintained at 37 ± 1°C. Samples of dissolution medium were removed at various time points, and after filtration, they were assayed for furosemide dissolved by measuring the absorbance at 271 nm employing Shimadzu Model UV 1800 spectrophotometer. The findings of dissolution studies are shown in Figure 2.

### X-ray diffraction

The powder X-ray diffraction studies of furosemide and complexes were studied employing X-ray powder diffractometer, PANalytical, Model No. × Pert pro employing Cu Kα radiation. The diffractograms were obtained between 2° and 40° at 2°/min in terms of 2 θ angle. A generator current of 30 mA at a generator tension (voltage) 40 kV was used. The diffractograms of furosemide and complexes are shown in Figure 3.

### Differential scanning calorimetry (DSC)

DSC studies were performed to know the physical nature of drugs in the prepared complex and to find out any interaction between furosemide and Captisol. The calorimeter (Shimadzu DSC 60+) was run at a scanning speed of 10°C/min. The temperature range of heating was 25–350°C. After sealing the samples in aluminum pans, heating was carried out in an inert atmosphere which is maintained by circulating nitrogen gas. The results of the DSC studies are shown in Figure 4.

### Fourier-transform infrared (FTIR) spectroscopy

The infrared spectroscopic analysis of furosemide and the complexes was performed by attenuated total reflectance sampling interface technique using Agilent Model Cary 630. Different spectra obtained are shown in Figure 5.

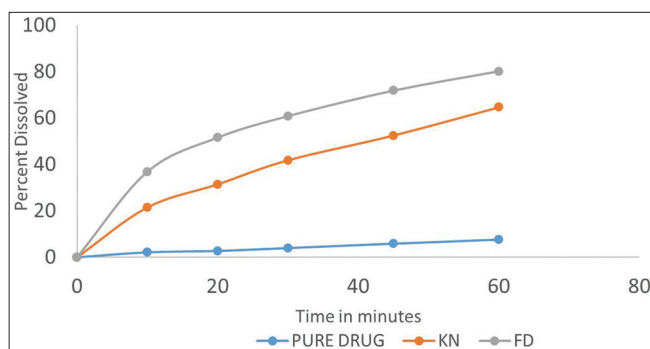


**Figure 2:** Dissolution profiles of pure drug furosemide and the inclusion complexes

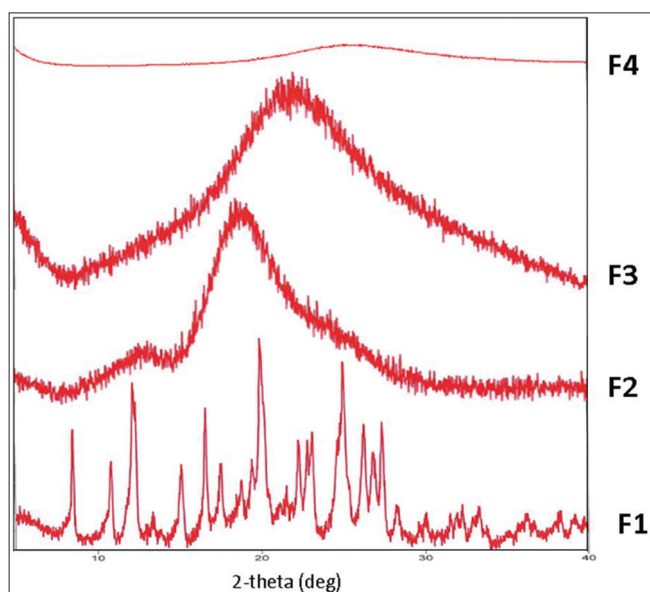


**Figure 3:** X-ray diffractograms of pure drug (F1); kneaded complex (F2); freeze-dried complex (F3), and sulfobutyl ether7-β-cyclodextrin (F4)

### Preparation of pellets by extrusion and spheronization

Exact quantities of FD complex and almond gum are mixed in a lab blender for 30 min (three levels of almond gum are employed [Table 1]. In case of F1 (4% almond gum), 96 g of complex and 4 g of almond gum are (total 100 g) were dry blended and then wet massed with water until a homogenous and cohesive mass is obtained. The mass was fed manually into extruder (Shakti model EX-50/SSP120) fitted with a die/screen of 1 mm diameter operated at a speed of 30 rpm. Spheronization was carried out in a unit fitted with crosshatched plate. Two spheronization speeds, 750 and 1200 rpm, were employed and operated for 6 min.

### Characterization of pellets

#### Determination of average pellet size

The pellet size of different formulations was estimated by sieve analysis (Electrolab Model EMS 8). Hundred grams

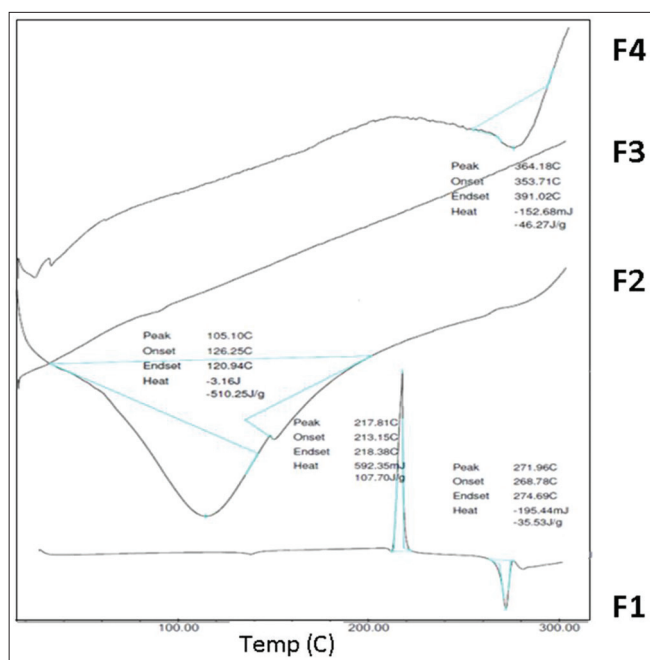


**Figure 4:** Differential scanning calorimetry of pure drug (F1); kneaded complex (F2); freeze-dried complex (F3) and sulfobutyl ether7- $\beta$ -cyclodextrin (F4)

of pellets were sieved employing a set of standard sieves. The sieve set was then mechanically shaken for 10 min. The net weight of pellets that is retained on each sieve was determined and these values were used for calculation of the average particle size.

### Friability, Carr's index, and angle of repose

#### Friability

The friability of the pellets was determined with a Roche friabilator operated for 10 min at 25 rpm. For each study, 25 g of pellets were mixed with 20 glass beads.

After passing the load through a sieve of mesh size 20, the weight of pellets left on the sieve was determined and the friability was calculated.

#### Carr's index

Hundred grams of pellets were added to a graduated cylinder and density apparatus (VTAP MATIC II). The bulk and tapped densities were determined. From the obtained values, the Carr's index and Hausner ratio were calculated.

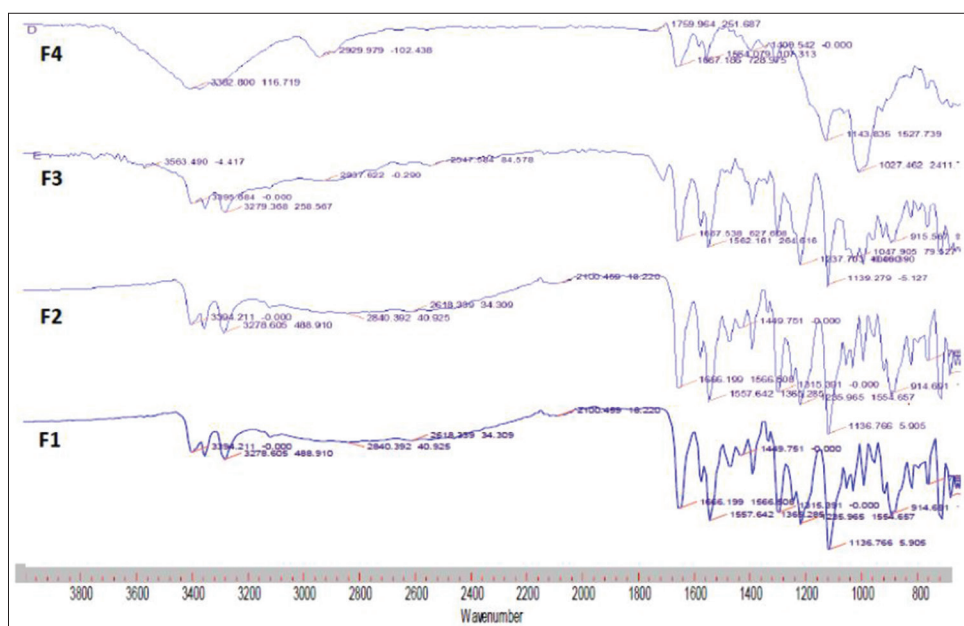


**Figure 5:** Fourier-transform infrared spectra of pure drug (F1); kneaded complex (F2); freeze-dried complex (F3), and sulfobutyl ether7- $\beta$ -cyclodextrin (F4)

**Table 1:** Details of different pellet formulations prepared

Formulation	Percentage of almond gum (%)	Speed of spheronization (rpm)	Size ( $\mu$ )
F1	4	750	640 $\pm$ 2.44
F2	8	750	812 $\pm$ 3.12
F3	16	750	1007 $\pm$ 2.89
F4	4	1200	872 $\pm$ 3.67
F5	8	1200	1122 $\pm$ 2.97
F6	16	1200	1305 $\pm$ 3.08

### Angle of repose

The angle of repose was measured according to the fixed funnel method.

### Surface characterization of pellets

The morphological observation was done by optical microscopic image analysis and scanning electron microscopy (SEM).

### Optical microscopy

The pellets were observed employing an Olympus microscope (Model BX 53) attached with DP 74 digital camera. The images were processed using cell sense software, as shown in Figure 6.

### SEM

The surface appearance and external features of the pellets were studied by employing SEM (Hitachi, Model SU 1510). After mounting the pellets onto a sample holder, they are observed under low pressure at an acceleration voltage of 15 kV. The SEM pictures of the pellets are shown in Figure 7.

### Drug release study

Release of furosemide from different pellets was studied by employing USP dissolution rate test apparatus Type I. 0.1 N hydrochloric acid for first 2 h and phosphate buffer of pH 7.4 for the remaining 10 h were used as medium for release study. Pellets containing 40 mg of furosemide are added to the drug release medium. The various removed samples of medium at different time points were assayed for furosemide released by determining the absorbance at 271 nm. The results are given in Table 2 and Figure 8.

## RESULTS AND DISCUSSION

### Phase solubility study

The phase solubility diagram of furosemide as a function of the concentration of SBE<sub>7</sub>-β-CD is shown in Figure 1. The

amount of furosemide soluble increased linearly with the amount of SBE<sub>7</sub>-β-CD. The slope of the line was <1 which indicated that the complex formed is in 1:1 molar ratio. The stability constant of the complex calculated was 1057 M<sup>-1</sup> which suggests that the complex will have good stability and dissolution required for high bioavailability. Complexes

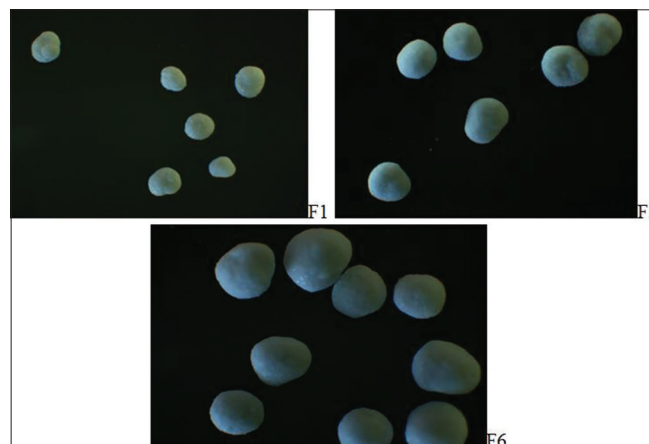


Figure 6: Photomicrographs of different pellets

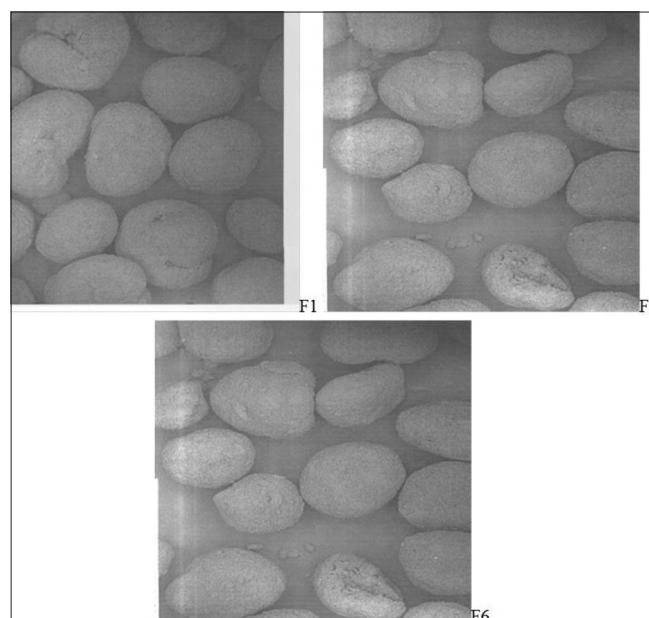
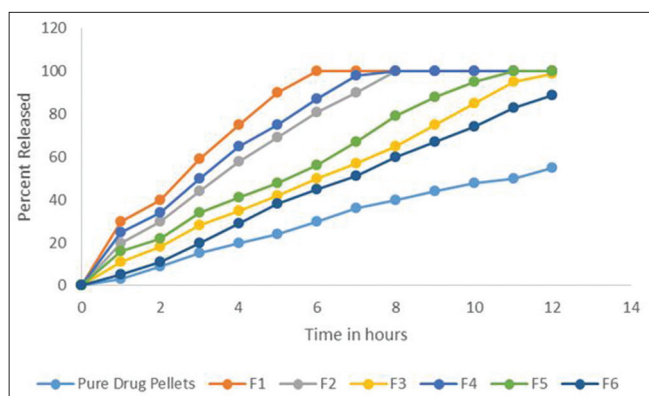


Figure 7: Scanning electron microscopy photographs of pellets

Table 2: Drug release characteristics of various pellet formulations

Formulation	Correlation coefficient (r <sup>2</sup> )			K <sub>1</sub>	K <sub>H</sub>	Korsmeyer–Peppas “n” value
	First-order	Higuchi	Korsmeyer			
F1	0.9717	0.9856	0.9335	0.4085	20.58	0.512
F2	0.9747	0.9842	0.9786	0.2881	18.93	0.579
F3	0.9629	0.9651	0.9917	0.1929	14.53	0.677
F4	0.9687	0.9881	0.9514	0.3208	18.89	0.538
F5	0.9824	0.9578	0.9871	0.2101	15.38	0.762
F6	0.9845	0.9708	0.9973	0.1683	14.21	0.806



**Figure 8:** Drug release profiles from various pellets

with very low or high stability constants are not useful for increasing absorption because they are too weak and very strong, respectively.<sup>[22]</sup>

### Characterization of furosemide and SBE<sub>7</sub>-β-CD inclusion complexes

#### Dissolution studies

The results of the dissolution studies of pure drug furosemide and the inclusion complexes are shown in Figure 2. It is observed that the complexes exhibited a rapid dissolution compared to the pure drug furosemide. In between the kneaded and FD complexes, the FD complex showed higher dissolution rate. At the end of 30 min, the pure drug showed <5% dissolution, the kneaded and FD complexes exhibited 39% and 62% dissolution, respectively. To assess the increase in dissolution, Khan has suggested the term dissolution efficiency (DE).<sup>[23]</sup> Pure furosemide showed DE<sub>30</sub> of 3.33% and the complexes showed 16.67% (KN) and 41.57% (FD). The K<sub>1</sub> values for the FD and kneaded complexes were higher (0.0264 min<sup>-1</sup> and 0.0161 min<sup>-1</sup>) compared to pure drug (0.0023 min<sup>-1</sup>). The extent of increase in dissolution observed from the complexes was assessed by finding out the difference (F1) and similarity factors (F2) as per the model proposed by Moore and Flanner.<sup>[24]</sup> The difference factor F1 is proportional to the average difference between the two profiles, whereas similarity factor F2 is inversely proportional to the average squared difference between the two profiles. In general, if the F1 values are above 15, then the two profiles compared are considered as different. In the present investigation, when the dissolution profile of pure drug is compared with the kneaded and FD complexes, the values are found to be 31.22 and 45.87, respectively.

#### Mechanism of increased dissolution from inclusion complex

To assess the cause of hike in the dissolution rate of furosemide from the prepared complexes, X-ray diffraction and DSC studies were carried out.

#### X-ray diffraction

The furosemide inclusion complexes were evaluated using X-ray diffraction [Figure 3]. Pure SBE<sub>7</sub>-β-CD showed no diffraction peaks suggesting its amorphous state. Similar observations are reported by other authors.<sup>[25]</sup> Pure drug furosemide exhibited sharp diffraction peaks indicating its crystalline nature, whereas the peaks have completely disappeared in the two complexes. This indicates that the crystalline drug is converted into an amorphous state in the complexes.

#### DSC

The endotherms of furosemide and the inclusion complexes are shown in Figure 4. The endotherm of furosemide showed two characteristic peaks. Initially, an exothermic peak at 217°C which is followed by an endothermic peak at 271°C. At 217°C probably furosemide underwent an exothermic process to set into a more stable equilibrium crystalline state which melted at 271°C. This polymorphic transition occurring in furosemide is reported by Patrycja and Marek.<sup>[26]</sup> In case of the inclusion complexes, the two peaks disappeared indicating that furosemide is no more in crystalline state but existed in amorphous solid solution state in the complex. This transformation into amorphous form and entrapment of the drug in the SBE<sub>7</sub> β-CD cavity of the complex explains why in the case of complexes the dissolution of furosemide is higher than that of the pure drug. In case of inclusion complex made by KN method broad endothermic peak can be seen at 105°C, which is probably because of the loss of residual moisture from the kneaded complex during the heating process.

Hence, the X-ray diffraction and DSC studies confirm the existence of furosemide in amorphous state in the inclusion complexes resulting in higher dissolution.

#### FTIR spectroscopy

FTIR spectroscopy was carried out to detect any chemical interaction between furosemide and SBE<sub>7</sub>-β-CD. Figure 5 illustrates the FTIR spectra of furosemide, SBE<sub>7</sub>-β-CD, and inclusion complexes. Characteristic bands for furosemide are observed at 3395 cm<sup>-1</sup> (N-H stretching vibration of Ar-NHCH<sub>2</sub> secondary amine), 3278 cm<sup>-1</sup> (N-H stretching), 1666 cm<sup>-1</sup> (C = O carboxylic acid stretching vibration of Ar-COOH), 1557 cm<sup>-1</sup> (-NH<sub>2</sub> bending vibration), and 1136 cm<sup>-1</sup> (symmetric SO<sub>2</sub>).<sup>[26]</sup>

All these characteristic bands are found to be retained in the two complexes. Thus, the IR spectra suggested that no chemical changes have taken place in furosemide during complexation.

#### Preparation and characterization of pellets

Pellets containing the inclusion complex were developed. In the present investigation, pellets were prepared by extrusion

and spheronization without the conventional and widely used spheronizing agent MCC. Almond gum is investigated as the spheronizing agent and also its usefulness to act as release retardant is studied. The influence of changing almond gum proportion and speed of spheronization on the properties of pellets formed and drug release is investigated.

The pellets are found to be spherical and free-flowing and exhibited satisfactory flow characteristics. The size of pellets ranged from 640 to 1305  $\mu$ . The details of different pellet formulations prepared are shown in Table 1 and their characteristics in Table 3. With changes in the percentage of almond gum and speed of spheronization, the size of the pellets could be varied. An increase in pellet size was observed with increase in the percentage of almond gum employed in the dry powder blend that was spheronized. For proper spheronization, the extruded mass must be sufficiently plastic and cohesive to result in uniform sized pellets. At the higher percentage of almond gum in the formulation, the extruded mass probably has more plasticity forming extruded strands of higher mechanical strength which after spheronization formed larger sized pellets with narrow size distribution. Furthermore, it is observed that a percentage of almond gum is increased, the pellets are found to be more spherical. As the spheronization speed is raised, the size of the pellets is found to be increased. This is in agreement with other reported works.<sup>[27,28]</sup> At lower speed of rotation of spheronizer sufficient frictional and rotational forces are not developed to convert the extrudates into well rounded off pellets. Hence, at lower speed probably, the pellets were being broken down before they were completely pelletized. The force and energy experienced by the pellets are determined probably by the speed employed in spheronization. This can influence the shape and size of pellets, as reported by Sin *et al.*<sup>[29]</sup>

Whereas less almond gum made the extruded mass less cohesive and more susceptible to be blown up into smaller pellets. In the case of formulation F1, where the percentage of almond gum is 4% and prepared at a spheronization speed of 750 rpm, the pellet size was 640  $\mu$  but in formulation F3 where the percentage was 16% operated at same speed the pellet size increased to 1007  $\mu$ . Whereas in case of formulation F4 in which case also the formulation contained same 4% almond gum but prepared at higher speed of spheronization, it resulted in pellet size of 872  $\mu$ . Hence, the percentage of almond gum and speed of spheronization influenced the size of pellets.

The surface features of pellets were investigated by optical microscopy and SEM. The pellets were found to be having smooth surface and well-rounded appearance [Figures 6 and 7]. However, it can be clearly noticed that pellets obtained at lower speed had irregular surface and are smaller in size. At higher spheronization rates, led to the formation of more regularly shaped larger sized pellets. The SEM photographs are shown in Figure 7. It can be seen that the pellets (F1) prepared employing lower percentage of almond gum and prepared at smaller speed of spheronization exhibited more irregularity and had surface features with cracks whereas pellets, F3 and F6, which are prepared with higher almond gum percentage and at higher speed of spheronization showed a smooth and regular surface features.

### Drug release

The drug release is found to be sustained and spread over a period of 12 h. The pellets with the inclusion complex of furosemide resulted in prompt release in the simulated gastric fluids which was not observed from pellets of pure drug furosemide (<10% in first 2 h). In case of formulations F1 and F2, the drug release is found to be more than the pure drug pellets but slow and sustained; however, in both the cases, the drug release is found to be complete by 7<sup>th</sup> h itself. This could be because of relatively smaller size of the pellets of F1 and F2 compared to F3. Hence, the higher surface area available from these pellets enabled drug to be released faster. Whereas in the case of formulation F3 with highest proportion of almond gum 16% and whose particle size is also high, the release is found to be much slower spread over complete 12 h. Thus, it can be seen that the drug could be varied with size of pellets and percentage of almond gum employed. A similar observation was made with respect to formulations F4, F5, and F6, which was prepared at higher spheronization speed and as such resulted in larger size pellets. In case of F6, it exhibited slowest release of all formulations (around 80%) at the end of 12 h.

To know the drug release mechanism – the data are analyzed as per first-order, Higuchi,<sup>[30]</sup> and Korsmeyer *et al.*<sup>[31]</sup> models. The model that best fits the release data was evaluated by correlation coefficient ( $r^2$ ). The  $r^2$  values in various models are given in Table 2.

**Table 3: Characteristics of different pellet formulations**

Formulation ( $\mu$ )	Average size ratio	Hausner	Carr index repose	Angle of (%)	Friability
F1	640 $\pm$ 2.44	1.15 $\pm$ 0.05	14.41 $\pm$ 1.15	25.21 $\pm$ 0.87	0.84 $\pm$ 0.09
F2	812 $\pm$ 3.12	1.23 $\pm$ 0.11	13.27 $\pm$ 0.92	27.18 $\pm$ 1.05	0.71 $\pm$ 0.11
F3	1007 $\pm$ 2.89	1.19 $\pm$ 0.21	16.34 $\pm$ 1.23	23.29 $\pm$ 0.93	0.57 $\pm$ 0.05
F4	872 $\pm$ 3.67	1.22 $\pm$ 0.17	15.89 $\pm$ 1.31	22.65 $\pm$ 1.17	0.77 $\pm$ 0.12
F5	1122 $\pm$ 2.97	1.09 $\pm$ 0.56	14.32 $\pm$ 0.87	26.67 $\pm$ 0.47	0.62 $\pm$ 0.08
F6	1305 $\pm$ 3.08	1.15 $\pm$ 0.21	15.51 $\pm$ 0.95	23.85 $\pm$ 1.29	0.52 $\pm$ 0.06

**Table 4:** Analysis of variance of the drug released from different pellet formulations

Source	Degrees of freedom	Sum of squares	Mean of squares	F value	P
Time (A)	11	157925.694	14356.881	33303.2075	<0.001
Percent drug released (B)	6	73657.987	12276.331	28477.0206	<0.001
Interaction (AB)	66	12073.087	182.926	424.3267	<0.001
Error	168	72.424	0.431		
Total	251	243729.193			

When the amount released was plotted against the square root of time, it gave straight lines with high  $r^2$  values indicating that the drug release is by diffusion. The release followed first-order kinetics because the correlation coefficient values are higher than for the zero-order. The  $n$  values of Peppas plot ranged between 0.512 and 0.806 suggesting the release is non-Fickian anomalous diffusion. Accordingly, the drug release from these pellets involves penetration by dissolution fluid, dissolution of the drug in dissolution fluid, and diffusion of the dissolved drug.

### Statistical analysis of drug release profiles

A statistical analysis is performed to compare the drug release profiles of various pellet formulations. Analysis of variance (ANOVA) was performed using two factors completely randomized design by employing MSTATC statistical analysis software. The results of ANOVA analysis for products are shown in Table 4.

According to the results of ANOVA, the percent released was found to be significantly different at each time level ( $P < 0.001$ ) and among the drug products ( $P < 0.001$ ), implying time with drug product interaction was highly significant (at  $P < 0.001$ ), i.e., that the release profiles were not parallel. This interaction indicated that the mean difference of percent released among different drug products was not constant at any two points of time considered. The calculated F value of treatment groups is greater than tabulated F value (at 0.01 level of probability). The results of ANOVA also showed that the drug products were significantly different in terms of percent released at each time point.

### CONCLUSION

The present study was taken up to determine the influence of formulation and processing factors on the drug release of furosemide pellets prepared by extrusion and spheronization. Drug release from pellets containing only the poorly soluble furosemide resulted in a poor release. Inclusion complexation of furosemide with sulfobutyl ether- $\beta$ -cyclodextrin resulted in increased dissolution. FD method gave a complex with higher dissolution than the KN method. The pellets of furosemide complex could be prepared employing almond gum without the need for the conventional spheronizing

agent MCC. With changes in the percentage of almond gum and speed of spheronization, the size of the pellets could be varied. As percentage of almond gum and speed of spheronization increased, the pellet size increased. With changes in almond gum percentage and size of pellets, extent of drug release also changed ( $F1 > F4 > F2 > F5 > F3 > F6$ ). Employing the inclusion complex of poorly soluble drugs for preparing SR pellets is a novel approach which ensures prompt but slow release in the gastric fluids.

### ACKNOWLEDGMENT

The authors express their gratitude to the President of RAK Medical and Health Sciences University, UAE and Dean RAK College of Pharmaceutical Sciences for their encouragement and support in carrying out the research.

### REFERENCES

1. Nowsheen G, Archana B. Naltrexone: A review of existing sustained drug delivery systems and emerging nano-based systems. *J Control Release* 2014;183:154-66.
2. Junyaprasert VB, Manwiwattanakul G. Release profile comparison and stability of diltiazem-resin microcapsules in sustained release suspensions. *Int J Pharm* 2008;352:81-91.
3. Tongkai C, Jian T. Multi-unit pellet system for controlled drug delivery. *J Control Release* 2017;262:222-31.
4. Javed I, Ranjha NM, Mahmood K, Kashif S, Rehman M, Usman F. Drug release optimization from microparticles of poly(E-caprolactone) and hydroxypropyl methylcellulose polymeric blends: Formulation and characterization. *J Drug Deliv Sci Tec* 2014;24:607-12.
5. Ghebre SI. Pellets: A general overview. In: Ghebre-Sellassie I, editor. *Pharmaceutical Palletization Technology*. New York: Marcel Dekker; 1989. p. 1-15.
6. Sandipkumar P, Nrupa P, Manju M, Abhijeet J. Controlled-release domperidone pellets compressed into fast disintegrating tablets forming a multiple-unit pellet system (MUPS). *J Drug Deliv Sci Technol* 2018;45:220-9.
7. Roblegg E, Ulbing S, Zeissmann S, Zimmer A. Development of lipophilic calcium stearate pellets using ibuprofen as a model drug. *Eur J Pharm Biopharm* 2010;75:56-62.

8. Okada S, Nakahara H, Isaka H. Adsorption of drugs on microcrystalline cellulose suspended in aqueous solutions. *Chem Pharm Bull* 1987;35:761-8.
9. Basit AW, Newton JM, Lacey LF. Formulation of ranitidine pellets by extrusion-spheronization with little or no microcrystalline cellulose. *Pharm Dev Technol* 1999;4:499-505.
10. Santos H, Veiga F, Pina ME, Sousa JJ. Compaction, compression and drug release characteristics of xanthan gum pellets of different compositions. *Eur J Pharm Sci* 2004;21:271-81.
11. Chatchawalsaisin J, Podczeck F, Newton JM. The influence of chitosan and sodium alginate and formulation variables on the formation and drug release from pellets prepared by extrusion/spheronisation. *Int J Pharm* 2004;275:41-60.
12. Verstraete G, Jaeghere WD, Vercruyssen J, Grymonpre W, Vanhoorne V, Stauffer F, *et al.* The use of partially hydrolysed polyvinyl alcohol for the production of high drug-loaded sustained release pellets via extrusion-spheronisation and coating: *In vitro* and *in vivo* evaluation *Int J Pharm* 2017;517:88-95.
13. Bouaziz F, Ben Romdhane M, Helbert CB, Buon L, Bhiri F, Bardaa S. Healing efficiency of oligosaccharides generated from almond gum (*Amygdalus communis*) on dermal wounds of adult rats. *J Tissue Viability* 2014;23:98-108.
14. Sarojini A, Kunam DS, Manavalan R, Jayanthi B. Effect of natural almond gum as a binder in the formulation of diclofenac sodium tablets. *Int J Pharm Sci Res* 2010;1:55-60.
15. Syed AH, Jaisankar V. An eco-friendly synthesis, characterization and antibacterial applications of novel almond gum-poly(acrylamide) based hydrogel silver nanocomposite *Polym Test* 2017;62:1016-29.
16. American Society of Health System Pharmacists. AHFS Drug Information. Bethesda, Maryland, USA: American Society of Health System Pharmacists; 2017. p. 28913.
17. Amidon GL, Lennerlas H, Shah VP, Crison JR. A theoretical basis for a biopharmaceutic drug classification: The correlation of *in vitro* drug product dissolution and *in vivo* bioavailability. *Pharm Res* 1995;12:413-20.
18. Jain AS, Date AA, Nagarsenker MS. Sulfobutyl ether(7)  $\beta$ -cyclodextrin (SBE(7)  $\beta$ -CD) carbamazepine complex: Preparation, characterization, molecular modeling, and evaluation of *in vivo* anti-epileptic activity. *AAPS PharmSciTech* 2011;12:1163-75.
19. Lockwood SF, O'Malley S, Mosher GL. Improved aqueous solubility of crystalline astaxanthin (3,3'-dihydroxy- $\beta$ ,  $\beta$ -carotene-4,4'-dione) by captisol® (sulfobutyl ether  $\beta$ -cyclodextrin). *J Pharm Sci* 2003;92:922-6.
20. Okimoto K, Rajewski RA, Uekama K, Jona JA, Stella VJ. The interaction of charged and uncharged drugs with neutral (HP- $\beta$ -CD) and anionically charged (SBE7- $\beta$ -CD)  $\beta$ -cyclodextrins. *Pharm Res* 1996;13:256-64.
21. Higuchi T, Connors A. Phase-solubility techniques. In: *Advances in Analytical Chemistry Instrumentation*. New York: Wiley Interscience; 1965. p. 117-211.
22. Carrier RL, Miller LA, Ahmed I. The utility of cyclodextrins for enhancing oral bioavailability. *J Control Release* 2007;123:78-99.
23. Khan KA. The concept of dissolution efficiency. *J Pharm Pharmacol* 1975;27:48-9.
24. Moore JW, Flanner HH. Mathematical comparison of dissolution profiles. *Pharm Technol* 1996;20:64-75.
25. Ribeiro LS, Ferreira DC, Veiga FJB. Physicochemical investigation of the effects of water-soluble polymers on vinpocetine complexation with  $\beta$  cyclodextrin and its sulfobutyl ether derivative in solution and solid state. *Eur J Pharm Sci* 2003;20:253-66.
26. Patrycja G, Marek W. DSC, FTIR and Raman spectroscopy coupled with multivariate analysis in a study of co-crystals of pharmaceutical interest. *Molecules* 2018;23:2136.
27. Cesar L, John R. Effect of different production variables on the physical properties of pellets prepared by extrusion-spheronization using a multivariate analysis. *Thai J Pharm Sci* 2017;41:69-75.
28. Kaisri U, Padungkwan C, Sukavat A. Influence of process variables on physical properties of the pellets using extruder and spheronizer. *Drug Dev Ind Pharm* 1999;25:45-61.
29. Sin YP, Hsiu NY, Cheng SC. Production and characterization of pellets using avicel CL611 as spheronization aid. *Drug Dev Ind Pharm* 2014;40:418-24.
30. Higuchi T. Mechanism of sustained action medication. Theoretical analysis of rate of release of solid drugs dispersed in solid matrices. *J Pharm Sci* 1963;52:1145-9.
31. Kormsmeier RW, Gurny R, Doelker E, Buri P, Peppas NA. Mechanisms of solute release from porous hydrophilic polymers. *Int J Pharm* 1983;15:25-35.

**Source of Support:** Nil. **Conflict of Interest:** None declared.